51. Primary Neoplasms

As with spinal central canal neoplasms in other regions, those of the lumbar spine may be classified as extradural, intradural extramedullary, and medullary. If an extradural lesion displaces the cord, the subarachnoid space (although it can be markedly compressed) will be present at the interface, with the thecal sac displaced away from the mass. In the lumbar spine, extradural lesions predominantly consist of vertebral body tumors and metastatic disease (see Chapter 49).

Nerve sheath tumors and meningiomas comprise the major neoplasms in the intradural extramedullary space. The major nerve sheath tumors are schwannomas and neurofibromas, the imaging appearances of which were discussed in Chapter 39. These lesions are somewhat less common in the lumbar spine as compared to the thoracic. Frequently affecting the nerve roots within the intervertebral foramina in the cervical and thoracic spine, schwannomas within the lumbar spine may also involve the roots of the cauda equina. Such an appearance is demonstrated in the T2 and CE T1WI of Figure 51.1 A, B, respectively. Schwannomas and neurofibromas are difficult to distinguish, even on MRI, although a heterogenous appearance on T2WI (as in the rather lobulated lesion of Figure 51.1) tends to favor the former. Schwannomas also occur peripheral to the nerve, tending to compress rather than enlarge it, more commonly exhibit cystic degeneration, and tend to be solitary rather than multiple.

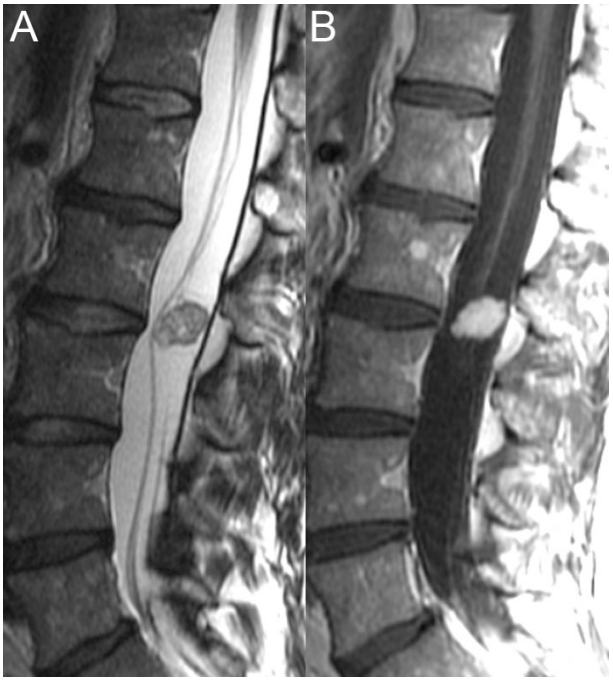

Fig 51.1

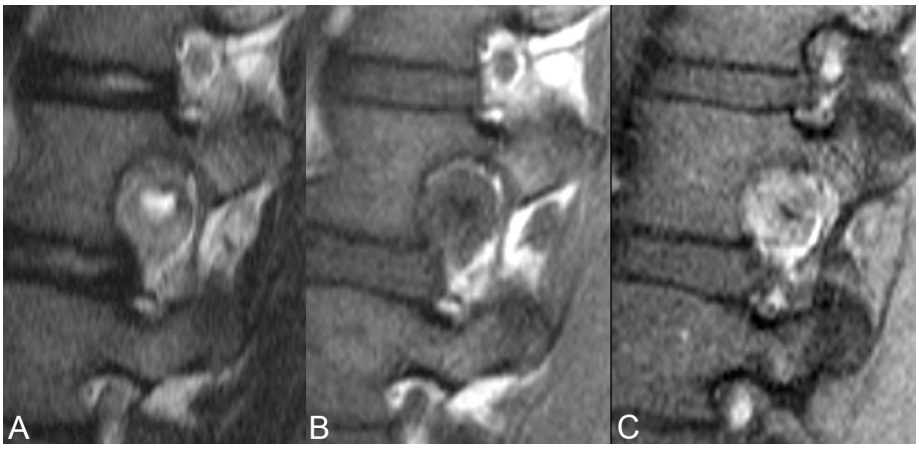

Fig. 51.2

Figure 51.2 A-C (T2, T1, CE T1WI) demonstrates a neurofibroma scalloping the posterior margin of the L2 vertebral body and widening the neural foramina in a patient with type 1 neurofibromatosis. On the basis of the illustrations presented here, this lesion could represent a schwannoma or neurofibroma, however, in this case two additional enhancing intrathecal lesions were seen, favoring the latter. Although cystic degeneration is seen on T2WI (A) as an area of central high SI, a more characteristic appearance (for a neurofibroma in the spine) is that of a target-like configuration on T2WI with a bright rim surrounding a center of low SI. A nerve sheath tumor in this location may be distinguished from a foraminal disk herniation by the presence of contrast enhancement. A plexiform neuroma—pathognomonic for type 1 neurofibromatosis—may occasionally be seen involving the sacral plexus as a bulky, lobulated, enhancing mass. Meningiomas are a further differential consideration with an intradural extramedullary mass. Unlike in the cervical spine, these tend to involve the posterolateral aspect of the canal in the thoracic and lumbar regions. The widened subarachnoid space above and below the lesion in Figure 51.3 A-C localizes it to the intradural extramedullary space. As with the aforementioned lesions, this meningioma demonstrates isointensity to the cord on precontrast T2 (A) and T1WI (B) images, most well-visualized on the former against the high SI CSF. (C) Contrast administration reveals characteristic prominent, homogenous enhancement due to tumor vascularity. Occasionally, flow voids on FSE T2WI may be seen along the periphery of particularly well-vascularized meningiomas. Dense calcification, resulting in low SI on all imaging sequences, is also common. The axial images of Figure 51.3 D demonstrate this meningioma to extend within the foramen.

Unlike the other predominately intramedullary tumor—astrocytomas—ependymomas frequently involve the lumbar spine and are the most common tumor of the conus, cauda equina, and filum terminale. In distinction to astrocytomas, their central, intramedullary

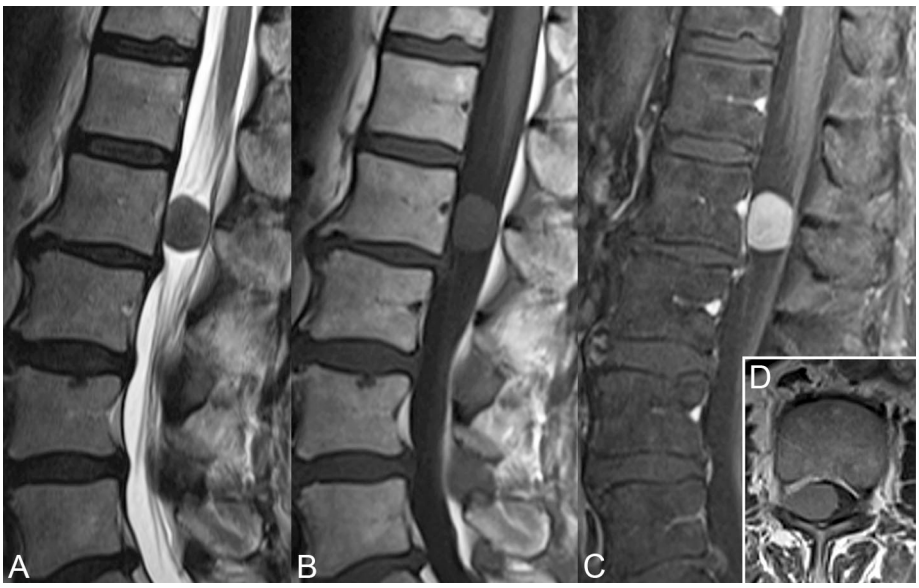

Fig. 51.3

location reflects their origin in the ependymal cells which line the CSF-containing central canal throughout the spinal cord. The lesion in Figure 51.4 A, B extends from L1 to L3, nearly filling the spinal canal and resulting in nerve root displacement. Its iso- to slight hyperintensity with the cord is punctuated by small foci of lower SI which may represent hemorrhagic components or areas of hypercellularity. Calcification may have a similar

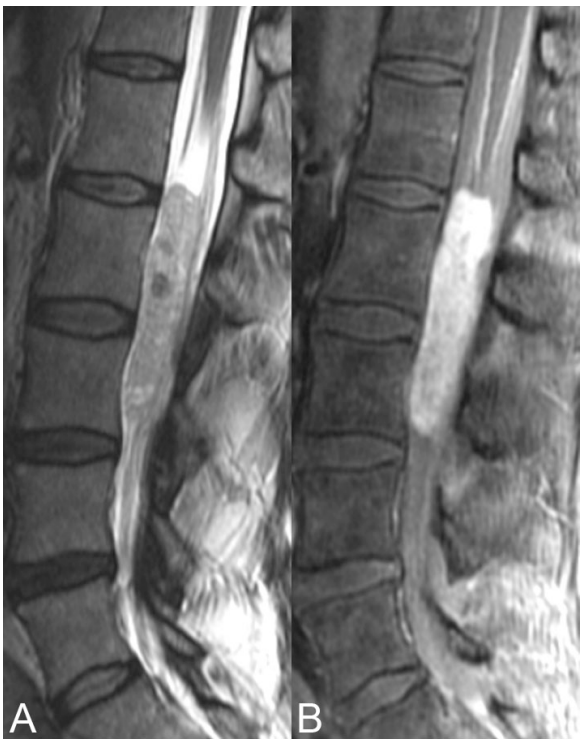

Fig. 51.4

appearance on T2WI, although this is much less common in spinal ependymomas versus those of the brain. Furthermore, the lack of corresponding low SI on post-contrast T1WI (B) makes calcification unlikely. The SI of this lesion on T2WI is actually slightly greater than that seen with the typical cellular-type of ependymoma. In fact, within the lower cord and especially in the area of the filum (90%), the myxopapillary subtype is more common, and the abundant mucinous secretions within the myxopapillary ependymoma in Figure 51.4 have resulted in a high SI appearance on

T2WI. Similarly, myxomatous lesions appear of higher SI than isointense (to the cord) cellular ependymomas on T1WI. Myxomatous lesions also tend to be larger and hemorrhage more frequently than their cellular counterparts. Both myxomatous and cellular subtypes enhance avidly but non-uniformly with such enhancement potentially outlining cystic areas of tumor which often appear isointense to CSF on other sequences. In this specific patient case, the additional enhancement surrounding the conus in Figure 51.4 B was felt likely to represent metastatic spread. At surgery, this was confirmed, along with involvement of and adherence to the nearby nerve roots. In addition to the aforementioned characteristics, ependymomas are distinguished from astrocytomas by their propensity to hemorrhage, to contain regions of low SI hypercellularity, and to have more precisely demarcated borders.

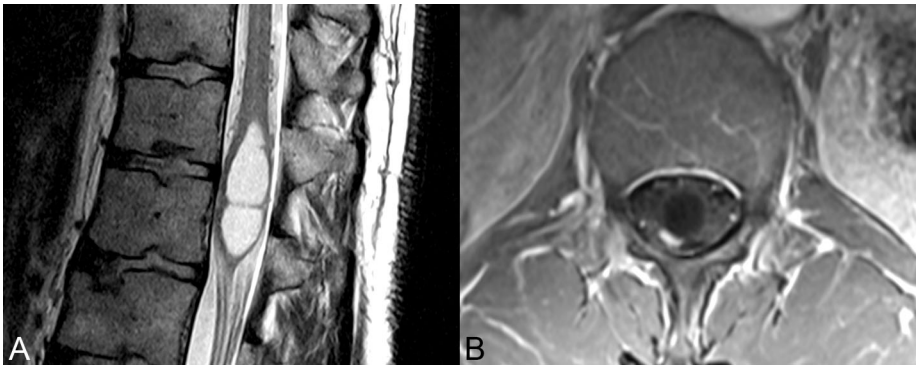

Fig. 51.5

Like the tumors previously discussed, hemangioblastomas also tend to be intramedullary, although they occur more frequently in the cervical and thoracic regions and are fairly rare in the spinal cord overall. Multiple cord hemangioblastomas are pathognomonic for von Hippel-Lindau (see Chapter 27). They may be solid or cystic in appearance, the latter more common for large intramedullary lesions and demonstrated in Figure 51.5 A, B. The SI of the cystic component varies, depending upon proteinaceous content. No nidus was readily identifiable on pre-contrast sequences in the patient case illustrated. While a large cystic metastasis could have a similar appearance, the presence of flow voids from dilated meningeal veins on FSE T2WI is nearly pathognomonic for hemangioblastoma. On (B) axial post-contrast T1WI, a brightly enhancing nidus is visible posterolaterally to the cystic component, emphasizing how small this area may be compared to the cystic component. Although not seen here, edema associated with a hemangioblastoma of the spinal cord may further complicate their distinction from metastatic lesions.

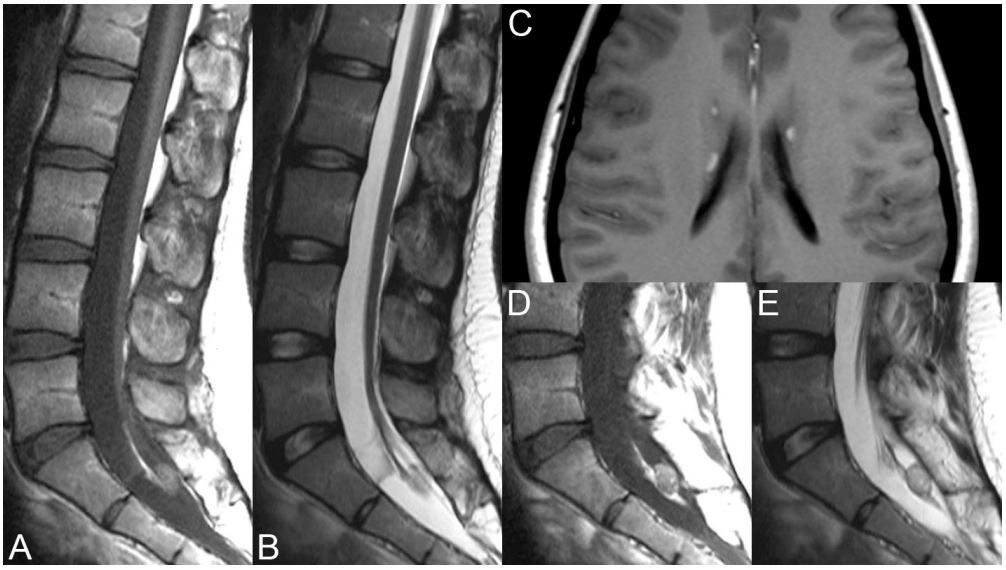

Fig. 51.6

A dermoid (or epidermoid) is a benign entity that may also appear as an intramedullary mass, most frequently in the lumbosacral region (Fig. 51.6). In this case (as best-seen in Fig. 51.6 A, B), the lesion is associated with a tethered cord—a congenital abnormality in which the conus is held in an abnormally low position. The appearance of this lesion, located at the termination of the thecal sac, on the respective T1 and T2WI of Figure 51.6 A, B is non-specific, but fat droplets in the subarachnoid space (in this instance along the periphery of the lateral ventricles) on axial T1WI of the brain (C) and additional sagittal spine images (D, E) clinches the diagnosis of a ruptured dermoid. Unlike an epidermoid, these lesions contain dermal appendages such as hair and sebaceous glands, secretions from the latter leading to the appearance of fat-like SI within the lesion. Fat droplets are present as foci of high SI within the ventricles of the brain on (C) T1WI, indicating dermoid rupture. The fat within the dermoid is seen as high SI on both the T1 and fast spin echo T2WI of Figure 51.6 D, E. A dermoid is reliably distinguished from a lipoma due to the absence of non-fat SI in the later.